

INFORMATION THEORETIC CRITERION BASED CLUTTER REDUCTION FOR GROUND PENETRATING RADAR

M. M. Riaz and A. Ghafoor*

Department of Electrical Engineering, College of Signals, National University of Sciences and Technology (NUST), Islamabad, Pakistan

Abstract—Singular value decomposition and information theoretic criterion based clutter reduction is proposed for ground penetrating radar imaging. The scheme is capable of discriminating target, clutter and noise subspaces. Information theoretic criterion is used with conventional singular value decomposition to find the target singular values. The proposed scheme also works for extracting multiple targets in heavy cluttered images. Simulation results are compared on the basis of mean square error, peak signal to noise ratio and visual inspection.

1. INTRODUCTION

Imaging of buried objects using Ground Penetrating Radar (GPR) is a challenging and open research area [1–3]. GPR is widely used (having applications in surveillance, remote sensing, geophysics, archaeology and civil engineering) because of its sensitivity to variations in electromagnetic parameters of a medium (i.e., electrical conductivity, electrical permittivity, and magnetic permeability). It can detect both metallic and non-metallic objects and is capable of localizing buried object(s) in two and three dimensional spaces [2].

The experimental GPR imaging system used in the experiments (shown in Figure 1) consists of an antenna, a Vector Network Analyzer (VNA), position controller and a signal processing unit (a computer) [2, 3]. The transmitter radiates a pulse into the ground and the receiver collects the echo for a certain time period. The transmitted pulse may be any transient signal (sine wave, step pulses, Gaussian wave etc.). Pulse widths are usually in the order of a

Received 8 August 2012, Accepted 19 October 2012, Scheduled 24 October 2012

* Corresponding author: Abdul Ghafoor (abdulghafoor-mcs@nust.edu.pk).

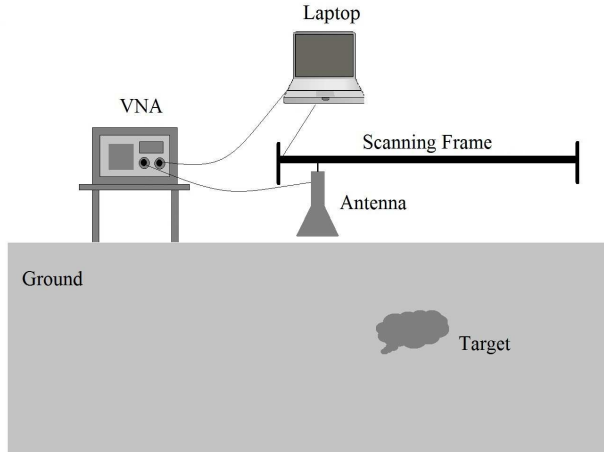


Figure 1. GPR experimental setup.

few nanoseconds [2]. A typical signal scattering in GPR is shown in Figure 2. Compared with conventional radar (where bandwidth of operation is limited to few (up to 200) KHz), GPR has broader bandwidth (normally in GHz for landmine detection) [2]. High frequencies provide high image resolution but have limited penetration depth and vice versa [2].

At a given location, the recorded pulse response is known as A-scan (magnitude of the reflected wave with respect to time). Due to propagation time, waves reflected from an object arrive at antenna of the GPR with a time delay (related to the distance between the object and the antenna of GPR). Image obtained by concatenating the A-scans (recorded at different spatial locations) is called a B-scan. Horizontal axis of a B-scan corresponds to the GPR spatial location, whereas the vertical axis corresponds to the time (which is linked with depth). A B-scan can be seen as an image of a vertical slice of the ground [3].

GPR received data is composed of target, clutter and noise signals [4, 5]. Detection of target(s) is a challenging task especially if the targets are buried close to the surface or have non-metallic characteristics (like antipersonnel mines). Clutter and noise are unwanted signals in the received data, caused by antenna coupling, air-ground reflection, scattering in the multi layer soil. Beside these, GPR also receives returns from other subsurface inhomogeneities like rocks, tree roots, or small pieces of metal in the ground, which leads to high levels of false alarms. The clutters and targets have overlapping

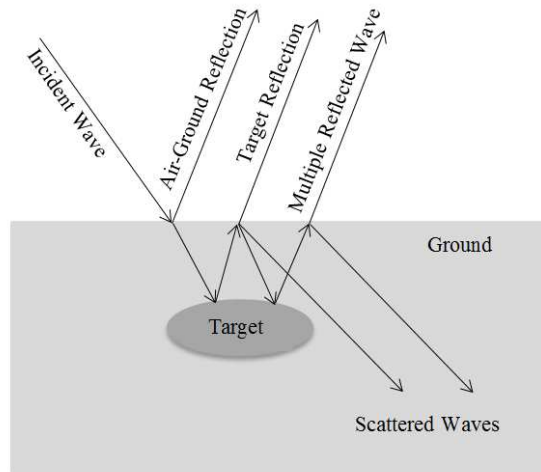


Figure 2. GPR signal reflection and scattering.

boundaries in time domain. A good GPR system should have minimum clutter and noise effect (to avoid false detection) and high resolution (to accurately classify target shape and location) [3].

Classical clutter reduction methods in GPR consists of data filtering in the time or frequency domain. A digital filter, whose coefficients are optimized with respect to the signal spectrum, is used for clutter reduction. However its limitation includes optimum selection of filter coefficients [6]. Another approach called early-time gating (which consists of eliminating early data samples of all traces) [7] is based on the assumption that the antenna coupling and surface reflections arrive early in time domain compared to the target signals. The early time gating fails to work for the cases where the target is buried close to the surface (or have same time response as surface reflection [7]). Frequency domain feature based approach [8] is also found in literature for clutter reduction and detection of land mines. However it fails to detect targets if the targets and clutter have overlapping response in the time domain.

Some other clutter reduction schemes consist of spatial modeling and subtracting the peak response due to the response of the airground interface [9,10]. However, these require accurate modeling of air-ground interface (which is not practically possible) and the performance of these methods degrade for non-homogenous mediums [9,10]. Another clutter reduction scheme uses adaptive linear prediction theory (to cancel the non stationary clutter environment) [11], however (its drawback is that) it makes the

assumption of Gaussian noise for the prediction error [11]. Parametric modeling based clutter reduction technique [12] assumes scattering from single target and neglects surface inhomogeneities. Neural network based clutter reduction techniques [13–15] require large input training data set. Maximum likelihood estimation [16], Markov model [17], Kalman filter [18] and whitening filter [19], are also present in literature for clutter reduction in GPR images. These schemes are based on hyperbolic signature of targets and require some a-priori knowledge of targets (which is not always present). Moreover, if the targets are buried close to the ground, the hyperbolic signature of target will be overlapped by ground reflections. Krichhoff approximation [20] and physical optic approximation [21] based techniques are also present for noise filtering.

Recently, statistical methods based on Singular Value Decomposition (SVD), principal component analysis and independent component analysis have been explored for clutter reduction [3, 22–29]. These methods explore the statistical properties of the received data and decompose it into different subspaces: target, clutter and noise. The components that contain targets are selected while discarding the noise and the clutter subspaces. The limitation is selection of target components by visual inspectio [22–29]. To overcome the problem of automatic selection of target subspaces, we propose a scheme based on Information Theoretic Criterion (ITC) and SVD. ITC is applied on singular values of B-scan image which gives the number of target subspaces that is used to construct the target image. Conventional SVD and the proposed ITC based SVD scheme are compared on the basis of Mean Square Error (MSE), Peak Signal to Noise Ratio (PSNR) and visual inspection.

In Section 2, we briefly explain the image reconstruction process. Section 3 describes existing and the proposed SVD based clutter reduction schemes. Simulation and results are discussed in Section 4 followed by the conclusion in Section 5.

2. IMAGE RECONSTRUCTION

Let the surface (to be imaged) is divided into grid of $M \times N$ pixels ($m = 1, 2, 3 \dots, M$ and $n = 1, 2, 3 \dots, N$). Let $\theta(t)$ be a wideband transmitted signal then the pixel value at location mn is,

$$\zeta_{mn}(t) = \vartheta(t + \hat{\tau}_{mn}) \quad (1)$$

where, $\hat{\tau}_{mn}$ are applied focusing delays and can be calculated by various methods depending on the available target information [2]. Received signal $\vartheta(t)$ is a delayed version of the transmitted signal $\theta(t)$ with some

attenuation α_{mn} , i.e.,

$$\vartheta_{mn}(t) = \alpha_{mn}\theta(t - \tau_{mn}) \quad (2)$$

where τ_{mn} are propagation time delays. Let $\hat{\theta}(t) = \theta(-t)$ be a filter matched to transmitted signal then the deconvolved output for pixel mn , x_{mn} is,

$$x_{mn} = \left(\zeta_{mn}(t) * \hat{\theta}(t) \right) \Big|_{t=0} = \left(\alpha_{mn}\theta(t - \tau_{mn} + \hat{\tau}_{mn}) * \hat{\theta}(t) \right) \Big|_{t=0} \quad (3)$$

The process (above) is repeated for each pixel location mn to obtain the B-scan image X .

$$X = \begin{bmatrix} x_{11} & x_{12} & \dots & x_{1N} \\ x_{22} & x_{22} & \dots & x_{2N} \\ \vdots & \vdots & \ddots & \vdots \\ x_{M1} & x_{M2} & \dots & x_{MN} \end{bmatrix} \quad (4)$$

3. SVD AND ITC BASED IMAGE ENHANCEMENT

Image enhancement in GPR is performed by decomposing the B-scan image X into different spectral components using SVD, i.e.,

$$X = USV^T = s_1 \begin{bmatrix} \vdots \\ u_1 \\ \vdots \end{bmatrix} [\dots v_1^T \dots] + \dots + s_M \begin{bmatrix} \vdots \\ u_M \\ \vdots \end{bmatrix} [\dots v_M^T \dots] \quad (5)$$

where (for simplicity $M \leq N$), $U = [u_1 u_2 \dots u_M]$ and $V = [v_1 v_2 \dots v_N]$ having dimensions $M \times M$ and $N \times N$ are called unitary matrices and computed as left XX^T and right $X^T X$ eigen vectors respectively. Let $S = \text{diag}(s_1, s_2, \dots, s_M)$ with $s_1 \geq s_2 \geq \dots \geq s_M \geq 0$, are singular values of X . The three spectral images clutter (X_{cl}), target (X_{tar}) and noise (X_{no}) of X are,

$$X = \sum_{m=1}^M X_m = \sum_{m=1}^{k_1} s_m u_m v_m^T + \sum_{m=k_1+1}^{k_2} s_m u_m v_m^T + \sum_{m=k_2+1}^M s_m u_m v_m^T \quad (6)$$

where the first k_1 singular values belong to ground clutters followed by $k_2 - k_1$ singular values belonging to target(s), and rest singular values represent noise. Abujarad, et al. [3, 28] proposed two algorithms for extraction of target spectral images. In first algorithm it was proposed that first spectral component contains ground clutters [3, 28], i.e.,

$$X_{cl1} = s_1 u_1 v_1^T \quad (7)$$

and the other components contain targets, i.e.,

$$X_{tar_1} = \sum_{m=2}^M s_m u_m v_m^T = X - X_{cl_1} \quad (8)$$

The limitation of this technique is that it only filters ground clutters while leaving the noise components unseparated. This results in poor visibility of targets specially when target shape and location are of interest. In second algorithm, [3, 28] proposed that ground clutters are contained in the first spectral components, target(s) are contained in the second spectral component while the rest spectral components contain noise, i.e.,

$$X_{tar_2} = s_2 u_2 v_2^T \quad (9)$$

However, we note that it is not true in case of multiple targets. In fact, the target subspace can be more than one dimensional even when only a single target is present in the scene. So we reformulate the above problem as,

$$\hat{X} = Y + Z = \sum_{m=2}^M s_m u_m v_m^T \quad (10)$$

where \hat{X} is the clutter reduced image, Y the target image, and Z the noise image. Since $rank[Y] = k_2 < M$, SVD of Y is, [30, 31],

$$Y = [U_{Y_1} \quad U_{Y_2}] \begin{bmatrix} S_{Y_1} & 0 \\ 0 & 0 \end{bmatrix} \begin{bmatrix} V_{Y_1}^T \\ V_{Y_2}^T \end{bmatrix} \quad (11)$$

where, $U_{Y_1}, U_{Y_2}, V_{Y_1}, V_{Y_2}$ are unitary matrices containing left and right singular vectors, and S_{Y_1} is a diagonal matrix containing singular value of Y . Therefore,

$$\begin{aligned} \hat{X} &= U_{Y_1} S_{Y_1} V_{Y_1}^T + Z = U_{Y_1} S_{Y_1} V_{Y_1}^T + Z V_{Y_2} V_{Y_2}^T \\ &= U_{Y_1} S_{Y_1} V_{Y_1}^T + Z [V_{Y_1} \quad V_{Y_2}] \begin{bmatrix} V_{Y_1}^T \\ V_{Y_2}^T \end{bmatrix} \\ &= [U_{Y_1} S_{Y_1} + Z V_{Y_1} Z V_{Y_2}] \begin{bmatrix} V_{Y_1}^T \\ V_{Y_2}^T \end{bmatrix} = [\hat{U}_1 \hat{U}_2] \begin{bmatrix} \hat{S}_1 & 0 \\ 0 & \hat{S}_2 \end{bmatrix} \begin{bmatrix} \hat{V}_1^T \\ \hat{V}_2^T \end{bmatrix} \end{aligned} \quad (12)$$

where $\hat{U}_1 = (U_{Y_1} S_{Y_1} + Z V_{Y_1}) (\hat{S}_{Y_1}^2 + \sigma_Z I_{k_2})^{-1/2}$, $\hat{U}_2 = Z V_{Y_2}$, $\hat{S}_1 = \sqrt{S_{Y_1}^2 + \sigma_Z I_{k_2}}$, $\hat{S}_2 = \sigma_Z I_{M-k_2}$, $\hat{V}_1^T = V_{Y_1}^T$, $\hat{V}_2^T = V_{Y_2}^T$, I_{k_2} is identity matrix of size $k_2 \times k_2$, I_{M-k_2} the identity matrix of size

$(I_{M-k_2}) \times (I_{M-k_2})$, and σ_Z the noise variance. The original image X in terms of clutter, target and noise subspaces is,

$$X = [u_1 \quad \hat{U}_1 \quad \hat{U}_2] \begin{bmatrix} s_1 & 0 & 0 \\ 0 & \hat{S}_1 & 0 \\ 0 & 0 & \hat{S}_2 \end{bmatrix} \begin{bmatrix} v_1^T \\ \hat{V}_1^T \\ \hat{V}_2^T \end{bmatrix} \quad (13)$$

where, \hat{S}_1 and \hat{S}_2 are diagonal matrices containing singular values of target $(s_2, s_3, \dots, s_{k_2})$ and noise $(s_{k_2+1}, s_{k_2+2}, \dots, s_M)$, respectively. Note that $s_{k_2} > s_{k_2+1}$ and $s_{k_2+1} \simeq s_{k_2+2} \simeq \dots \simeq s_M \simeq \sigma_Z$. Therefore, some statistical analysis needs to be performed in order to determine value for k_2 . In this regard some schemes in literature include difference of singular values $(s_m - s_{m+1})$, ratio of singular values (s_m/s_{m+1}) and percentage of total power in an singular value $(s_m/tr[X])$ [32]. However, these schemes do not always provide



Figure 3. Physical elements of experimental setup at Microwave Engineering Lab, Department of Electrical Engineering, College of Signals, NUST.

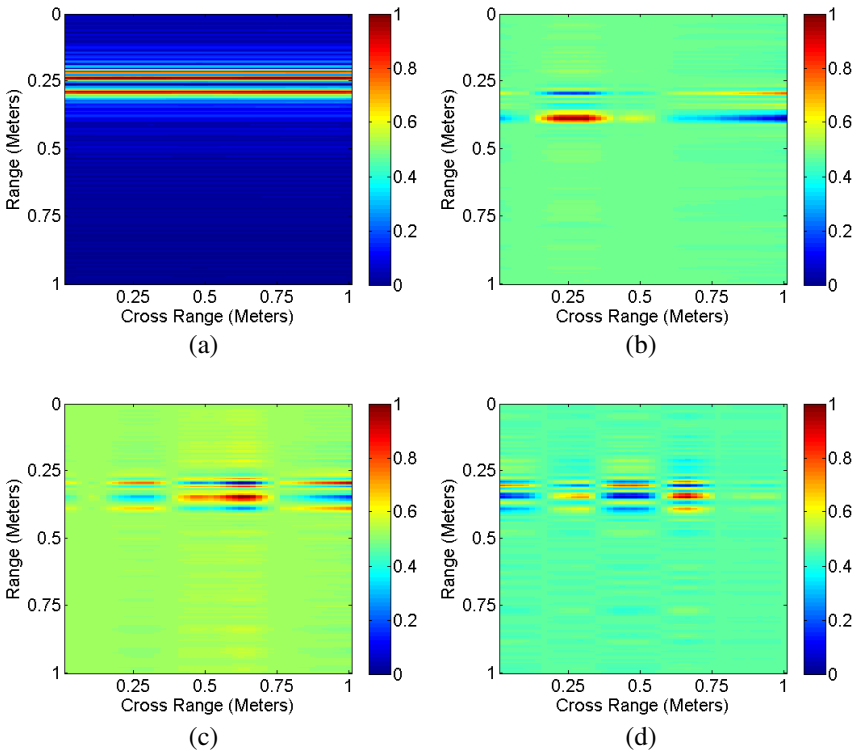
Table 1. MSE and PSNR (dB) comparison.

Scenarios	Techniques	MSE	PSNR
Example 1	Original Image	0.4866	3.1283
	Abujarad, et al. Technique I [3]	0.2731	5.6368
	Abujarad, et al. Technique II [3]	0.1549	8.0995
	Proposed Technique	0.1134	9.4539
Example 2	Original Image	0.4914	3.0856
	Abujarad, et al. Technique I [3]	0.3127	5.0487
	Abujarad, et al. Technique II [3]	0.1866	7.2909
	Proposed Technique	0.1325	8.7778

satisfactory results (and sometimes do not overcome the requirement of user defined threshold). It is observed that the difference between noise singular values are relatively smaller than target singular values. To accurately determine the number of target singular values ITC methods (Minimum Description Length (MDL), Bayesian information criterion and Akaike Information Criterion (AIC), etc.) are explored. MDL is an improved version of AIC [33], therefore MDL is chosen for finding the value of k_2 . ITC does not require knowledge of an empirical threshold value.

MDL utilizes measures of the relative cross entropy between target and noise singular values [33].

$$MDL(k_2) = N \ln \left[\frac{\left[\frac{1}{M-(k_2+1)} \sum_{m=k_2+1}^M s_m \right]^{M-(k_2+1)}}{\prod_{m=k_2+1}^M s_m} \right] + \frac{1}{2} k_2 (2M - k_2) \ln N \quad (14)$$



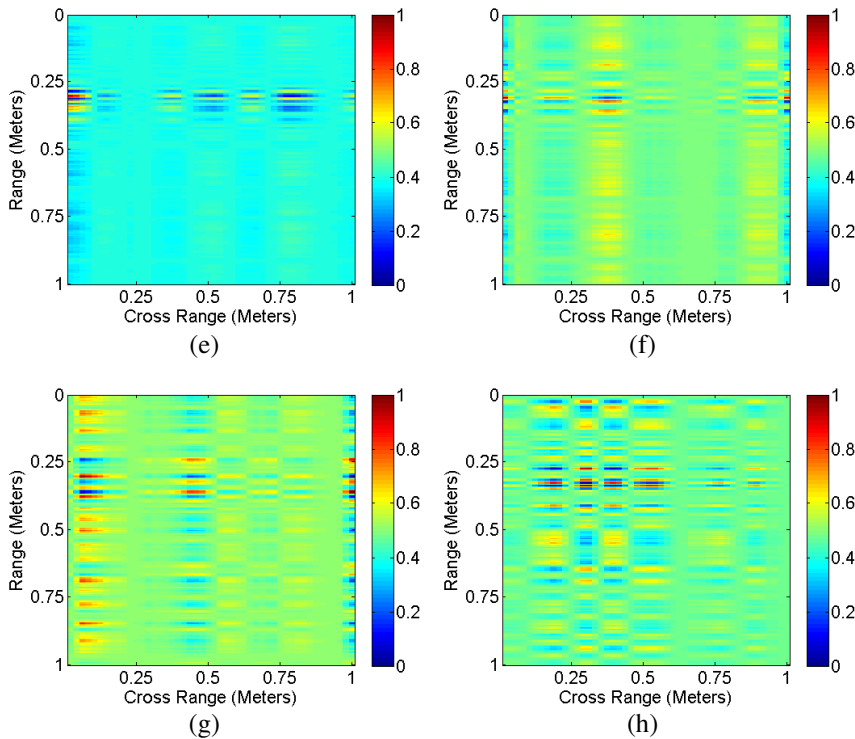


Figure 4. Presence of two targets in different spectral components. (a) First spectral component. (b) Second spectral component. (c) Third spectral component. (d) Fourth spectral component. (e) Fifth spectral component. (f) Sixth spectral component. (g) Seventh spectral component. (h) Eighth spectral component.

Number of target singular values is determined by the value of k_2 for which MDL criterion is minimized, i.e., $k_2^{\text{MDL}} = \underset{k_2}{\text{argmin}}\{\text{MDL}(k_2)\}$.

$$X_{tar_3} = \sum_{m=2}^{k_2^{\text{MDL}}} s_m u_m v_m^T \tag{15}$$

MDL works on the inequality of geometric and arithmetic mean of the singular values.

$$\frac{1}{M - (k_2 + 1)} \sum_{m=k_2+1}^M s_m \geq \left(\prod_{m=k_2+1}^M s_m \right)^{\frac{1}{M - (k_2 + 1)}} \tag{16}$$

In Eq. (16) equality holds only if $s_{k_2+1} = s_{k_2+2} = \dots = s_M$. As a consequence MDL criterion is minimized [33]. Note here that for noise only singular values $s_{k_2+1} \simeq s_{k_2+2} \simeq \dots \simeq s_M \simeq \sigma_Z$ the above equality holds (where, σ_Z is noise variance).

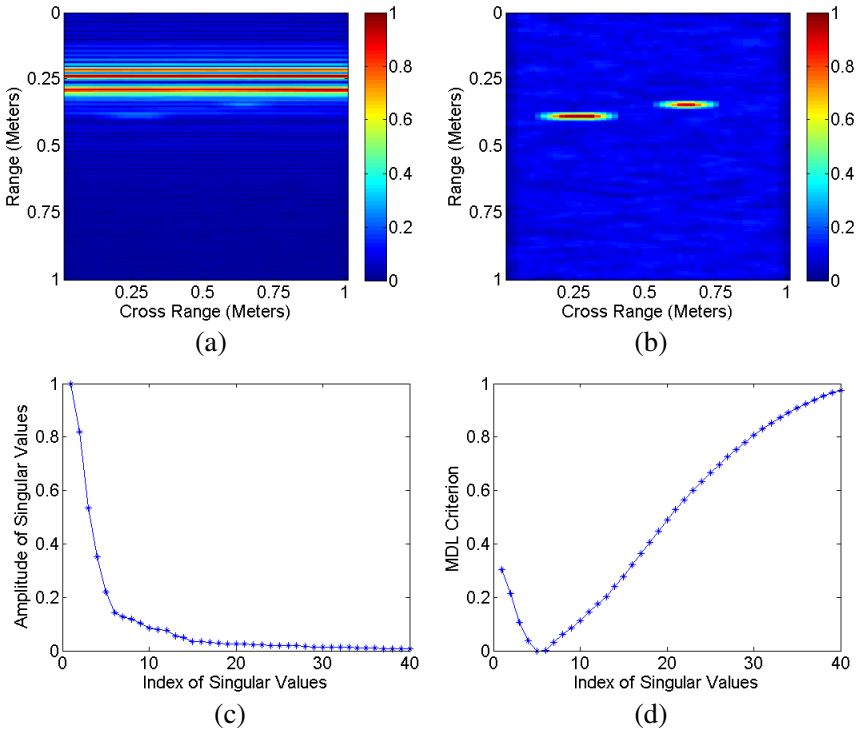
4. SIMULATION AND RESULTS

Various experiments were conducted to verify the effectiveness of proposed scheme. Experimental setup for GPR shown in Figure 3 Agilent's VNA in the range of 300 KHz to 3 GHz is used to generate a stepped frequency 2 GHz to 3 GHz (1 GHz Band Width (BW)) waveform having step size $\Delta f = 5$ MHz and $N_f = 200$. The pulse width is $T_P = 1/BW = 1$ ns. Maximum range R_{\max} is,

$$R_{\max} = \frac{c(N_f - 1)}{2BW} = 30 \text{ m}$$

and the range resolution ΔR is,

$$\Delta R = \frac{c}{2N_f\Delta f} = 0.15 \text{ m}$$



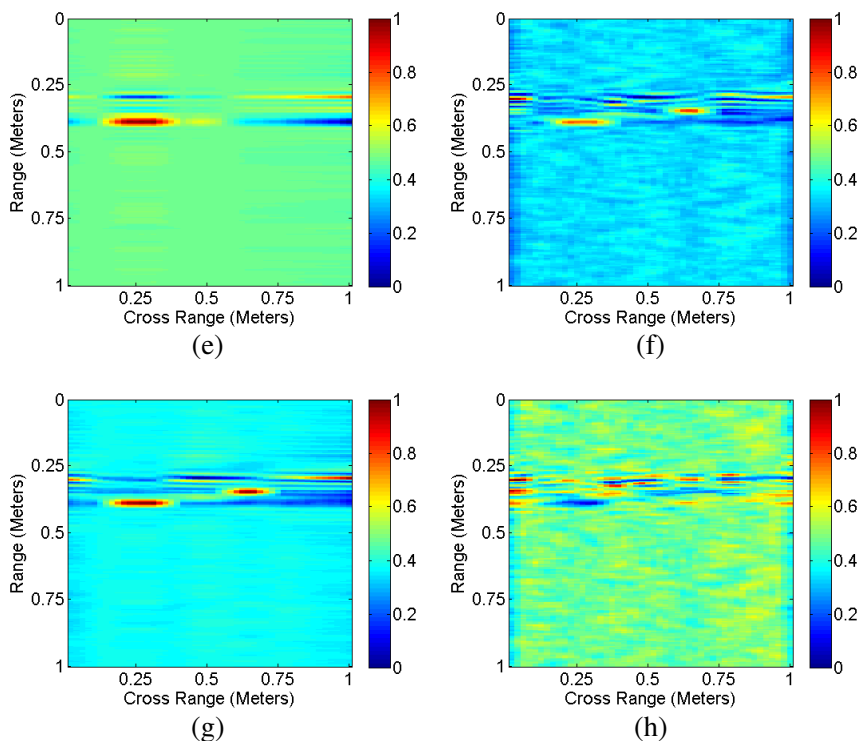


Figure 5. Images (original, Background subtracted reference Abujarad et al. technique I [3], Abujarad et al. technique II [3], proposed technique and noise subspace) with two targets and their related graphs (singular values and MDL function of singular values). (a) Original image. (b) Background subtracted reference image. (c) Amplitude of singular values. (d) MDL function of singular values. (e) Abujarad et al. technique I [3]. (f) Abujarad et al. technique II [3]. (g) Proposed technique. (h) Noise subspace.

Directional and broadband horn antenna with 12 dB gain is used in mono-static mode (for transmitting and receiving signals). Antenna is mounted on a robotic car which is controlled by a micro-controller and at each point the scattering parameters (magnitude and phase) are recorded by VNA and are transferred to a local computer. The antenna is positioned 0.0508 meters above the ground. Some targets are buried near the air ground surface to verify the effectiveness of proposed scheme when target and clutter have overlapping signatures in the time domain. Received data is converted from frequency domain to time domain using the inverse fourier transform. Background subtracted reference image X_{bs} is constructed using the difference of two images

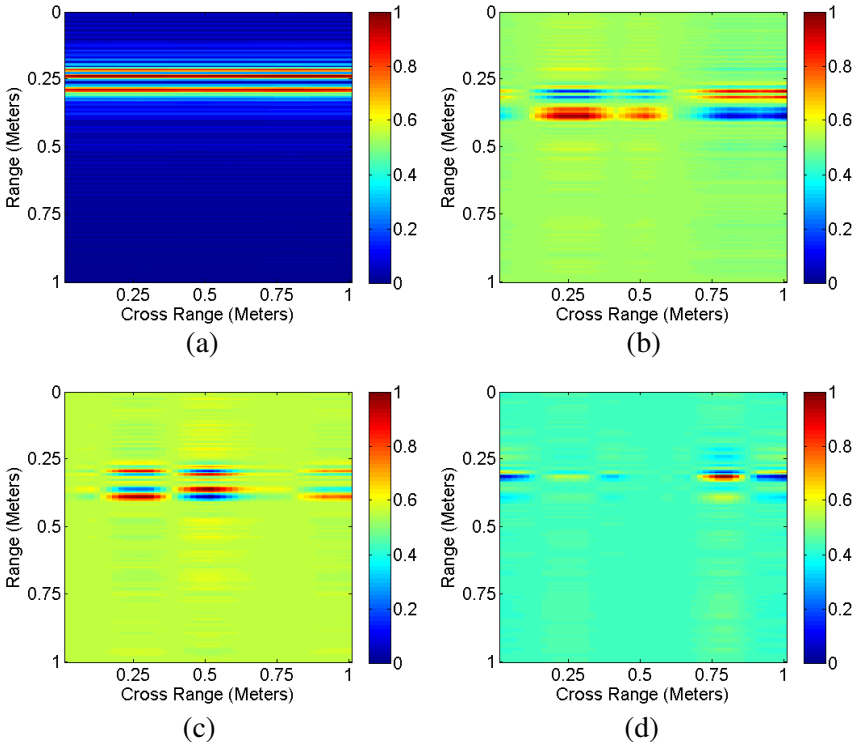
(i.e. image with target and image without target). It is important to note that the X_{bs} is used only as a comparison measure for proposed and existing SVD algorithms. Simulation results are compared on the basis of MSE, PSNR and visual inspection.

$$\text{MSE} = \frac{1}{M \times N} \sum_{m=1}^M \sum_{n=1}^N (X_{bs}(m, n) - X_{tar}(m, n))^2 \quad (17)$$

$$\text{PSNR (dB)} = 10 \log_{10} \frac{1}{\text{MSE}} \quad (18)$$

where, $X_{tar} \in \{X, X_{tar_1}, X_{tar_2}, X_{tar_3}\}$.

In example 1, two targets (metallic lock and metallic keys with non metallic coating) were buried in sand at different depths (0.1524 meters and 0.1016 meters respectively). Figure 4 shows different spectral components. It is observed that targets are not limited to the second spectral component only. Rather some part of the targets are also present in other spectral components. Figure 5 shows comparison of existing and proposed SVD based clutter reduction techniques. Figure 5(a) shows a B-scan image with two targets in it. Figure 5(b) shows the X_{bs} and Figure 5(c) shows the amplitude of singular values



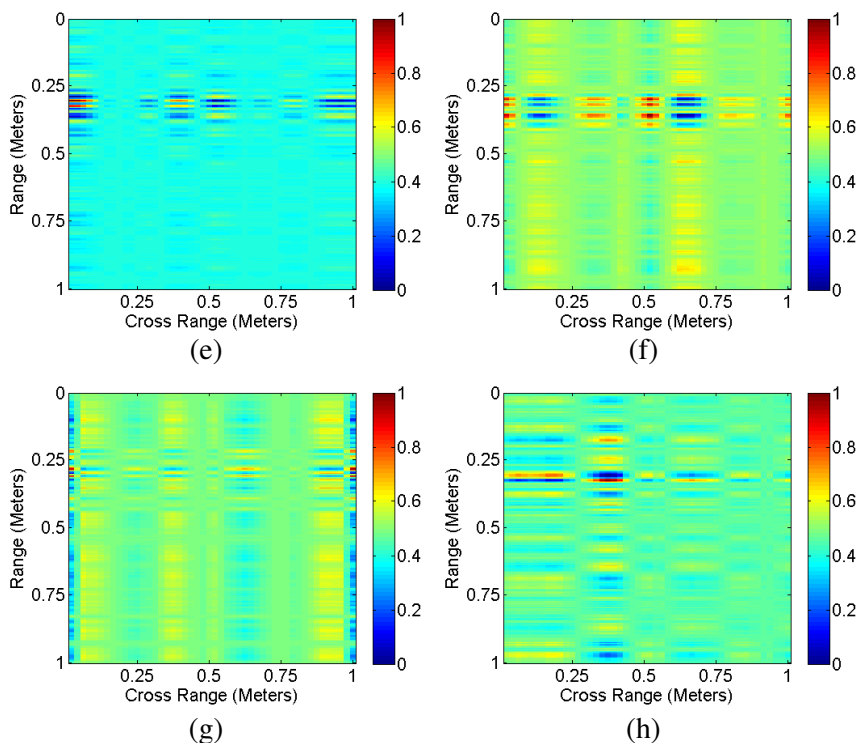


Figure 6. Presence of three targets in different spectral components. (a) First spectral component. (b) Second spectral component. (c) Third spectral component. (d) Fourth spectral component. (e) Fifth spectral component. (f) Sixth spectral component. (g) Seventh spectral component. (h) Eighth spectral component.

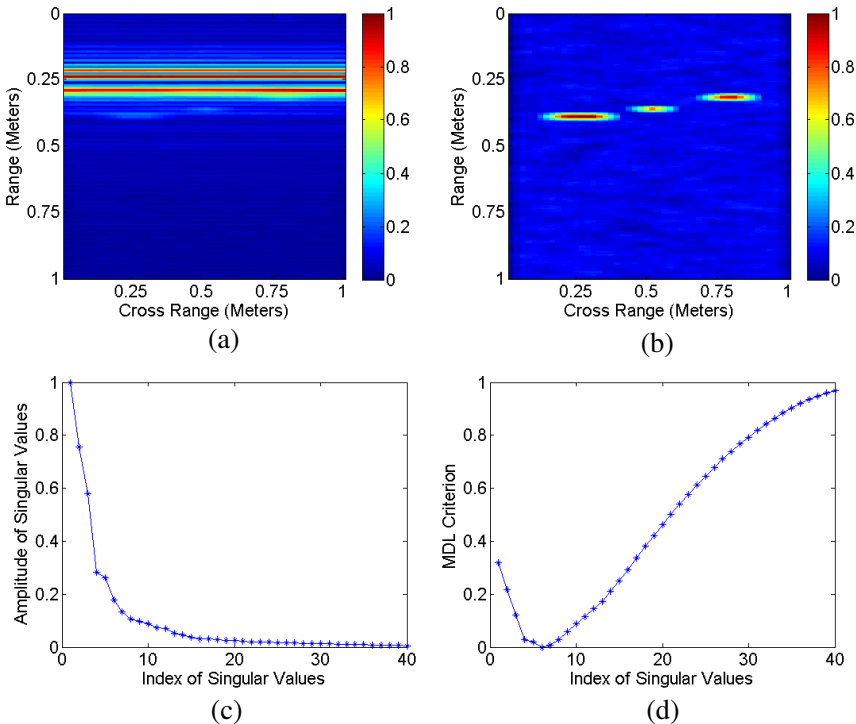
s_m . MDL criterion gives $k_2 = 5$ from Figure 5(d). Figure 5(e) and Figure 5(f) show the images obtained using Abujarad et al. techniques I and II [3] respectively. Figure 5(g) shows the image obtained using the proposed technique. Figure 5(h) shows the noise subspace obtained using the proposed scheme. It can be seen that image obtained using the proposed scheme show the targets clearly and eliminates the noise, whereas the false alarms are clearly visible in the images obtained using Abujarad et al. techniques [3].

In example 2, three targets (metallic lock, dummy mine and metallic keys with non metallic coating) were buried in sand at different depths (0.1524 meters, 0.1254 meters and 0.0812 meters respectively). Figure 6 shows the different spectral components. It is observed that the targets are not limited to the second spectral component only. Rather some part of the targets are also present in other

spectral components. Figure 7(a) shows a B-scan image with three target in it. Figure 7(b) shows the X_{bs} and Figure 7(c) shows the amplitude of singular values s_m . MDL criterion gives $k_2 = 6$ from Figure 7(d). Figure 7(e) and Figure 7(f) show the images obtained using Abujarad et al. techniques I and II [3] respectively. Figure 7(g) shows the image obtained using the proposed technique. Figure 7(h) shows the noise subspace obtained using proposed scheme. It can be seen that image obtained using the proposed scheme show the targets clearly and eliminates the noise, whereas false alarms are clearly visible in the images obtained using Abujarad et al. techniques [3].

Table 1 shows the performance comparison of proposed and Abujarad, et al. techniques in terms of MSE and PSNR.

Note that ITC is applied on the singular values of the B-scan image. SVD will change with the change in the input image, consequently it changes ITC (MDL) graph. Also, it is important to note that, it is not only the number of targets that determine the value of k_2 , rather it is the location, shape, size and reflectiveness of targets also. In some cases a single target may depend on more than one singular value. On the other hand, it is also possible that a singular value represents more than one target. However, the image formed by



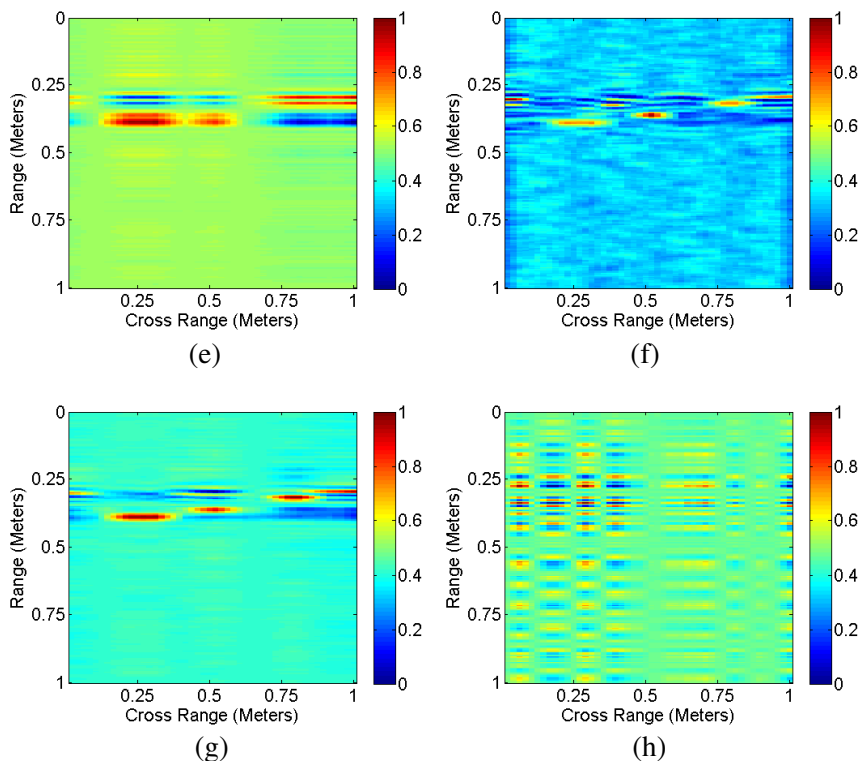


Figure 7. Images (original, Background subtracted reference, Abujarad et al. technique I [3], Abujarad et al. technique II [3], proposed technique and noise subspace) with three targets and their related graphs (singular values and MDL function of singular values). (a) Original image. (b) Background subtracted reference image. (c) Amplitude of singular values. (d) MDL function of singular values. (e) Abujarad, et al. technique I [3]. (f) Abujarad et al. technique II [3]. (g) Proposed technique. (h) Noise subspace.

using the k_2 (obtained via MDL) exactly extracts all the targets and suppresses the noise significantly.

5. CONCLUSION

SVD and ITC based clutter reduction technique is proposed for GPR imaging. The scheme is capable of discriminating target, clutter and noise subspaces. ITC is used with conventional SVD to find the target singular values. The proposed technique also works for extracting multiple targets in heavy cluttered images. Simulation

results show that the proposed technique is a significant improvement in conventional SVD based clutter reduction technique for GPR.

REFERENCES

1. Romano, N., G. Prisco, and F. Soldovieri, "Design of a reconfigurable antenna for ground penetrating radar applications," *Progress In Electromagnetics Research*, Vol. 94, 1–18, 2009.
2. Daniels, D. J., *Ground Penetrating Radar*, IEE, U.K., 2004.
3. Abujarad, F., "Ground penetrating radar signal processing for landmine detection," Ph.D. Thesis, 2007.
4. Oguz, U. and L. Gurel, "Frequency response of ground penetrating radars operating over highly lossy grounds," *IEEE Transactions on Geoscience and Remote Sensing*, Vol. 40, No. 6, 1385–1394, 2002.
5. Gurel, L. and U. Oguz, "Simulations of ground-penetrating radar over lossy and heterogeneous grounds," *IEEE Transactions on Geoscience and Remote Sensing*, Vol. 39, No. 6, 1190–1197, 2001.
6. Potin, D., E. Duflos, and P. Vanheeghe, "Landmines ground-penetrating radar signal enhancement by digital filtering," *IEEE Transactions on Geoscience and Remote Sensing*, Vol. 44, No. 9, 2393–2406, 2006.
7. Rahman, M. and K. B. Yu, "Total least squares approach for frequency estimation using linear prediction," *IEEE Transactions on Acoustics, Speech, Signal Processing*, Vol. 35, 1440–1545, 1987.
8. Ho, K. C., P. D. Gader, and J. N. Wilson, "Improving landmine detection using frequency domain features from ground penetrating radar," *IEEE Geoscience and Remote Sensing Symposium*, Vol. 3, 1617–1620, 2004.
9. Gupta, I. J., A. V. Merwe, and C. C. Chen, "Extraction of complex resonances associated with buried targets," *SPIE Detection Remediation Technology Mines and Mine-Like Targets III*, Vol. 3392, 568–580, Jul. 1997.
10. Carevic, D. D., M. Craig, and I. Chant, "Modelling GPR echoes from land mines using linear combination of exponentially damped sinusoids," *SPIE Detection Remediation Technology Mines and Mine-Like Targets II*, Vol. 3079, 1022–1032, Sep. 1998.
11. Farina, A. and A. Protopa, "New results on linear prediction for clutter cancellation," *IEEE Transactions on Aerospace and Electronic Systems*, Vol. 24, No. 3, 275–285, 1998.
12. Merwe, A. V. and I. J. Gutpa, "A novel signal processing

- technique for clutter reduction in GPR measurements of small, shallow land mines,” *IEEE Transactions on Geoscience and Remote Sensing*, Vol. 38, No. 6, 2627–2637, 2000.
13. Gamba, P. and S. Lossani, “Neural detection of pipe signature in ground penetrating radar images,” *IEEE Transactions on Geoscience and Remote Sensing*, Vol. 38, No. 2, 790–797, 2000.
 14. Vicen-Bueno, R., R. Carrasco-Alvarez, M. Rosa-Zurera, and J. C. Nieto-Borge, “Sea clutter reduction and target enhancement by neural networks in a marine radar system,” *Sensors*, Vol. 9, 1913–1936, 2009.
 15. Vicen-Bueno, R., M. Rosa-Zurera, M. P. Jarabo-Amores, and R. Gil-Pita, “Automatic target detection in simulated ground clutter (Weibull distributed) by multilayer perceptrons in a low-resolution coherent radar,” *IET Radar, Sonar, and Navigation*, Vol. 4, 315–328, 2010.
 16. Ho, K. and P. D. Garder, “A linear prediction landmine detection algorithm for hand held ground penetrating radar,” *IEEE Transactions on Geoscience and Remote Sensing*, Vol. 40, No. 6, 1374–1384, 2002.
 17. Gader, P. D., M. Mystkowski, and Y. Zhao, “Landmine detection with ground penetrating radar using hidden Markov models,” *IEEE Transactions on Geoscience and Remote Sensing*, Vol. 39, No. 6, 1231–1243, 2001.
 18. Zoubir, M., I. J. Chant, C. L. Brown, B. Barkat, and C. Abeynayake, “Signal processing techniques for landmine detection using impulse ground penetrating radar,” *IEEE Sensors Journal*, Vol. 2, 41–51, 2002.
 19. Dogaru, T. and L. Carin, “Time domain sensing of targets buried under a rough air-ground interface,” *IEEE Transactions on Antenna and Propagation*, Vol. 46, 360–372, 1998.
 20. Liseno, A., F. Tartaglione, and F. Soldovieri, “Shape reconstruction of 2-D buried objects under a Kirchhoff approximation,” *IEEE Geoscience and Remote Sensing Letters*, Vol. 1, 118–121, 2004.
 21. Pierri, R., A. Liseno, R. Solimene, and F. Soldovieri, “Beyond physical optics SVD shape reconstruction of metallic cylinders,” *IEEE Transactions on Antenna and Propagation*, Vol. 45, 655–665, 2006.
 22. Cagnoly, B. and T. J. Ulrych, “Singular value decomposition and wavy reflections in ground-penetrating radar images of base surge deposits,” *Journal of Applied Geophysics*, Vol. 48, No. 3, 175–182, 2001.

23. Karlsen, B., B. D. Sorensen, J. Larsen, and K. B. Jakobson, "Independent component analysis for clutter reduction in ground penetrating radar data," *SPIE Aerosense*, Vol. 4742, 378–389, 2002.
24. Kabourek, V., P. Cerny, and M. Mazanek, "Clutter reduction based on principal component analysis technique for hidden objects detection," *Radioengineering*, Vol. 21, 464–470, 2012.
25. Karlsen, B., B. D. Sorensen, J. Larsen, and K. B. Jakobson, "GPR detection of buried symmetrically shaped mine-like objects using selective independent component analysis," *SPIE Detection Remediation Technology Mines and Mine-Like Targets Aerosense*, Vol. 5089, 375–386, 2003.
26. Karlsen, B., J. Larsen, B. D. Sorensen, and K. B. Jakobsen, "Comparison of PCA and ICA based clutter reduction in GPR systems for anti-personal landmine detection," *11th IEEE Signal Processing Workshop on Statistical Signal Processing*, 146–149, 2001.
27. Ebihara, S., "Blind separation for estimation of near-surface interface by GPR with time-frequency distribution," *IEICE Transactions on Communications*, Vol. E86-B, 3071–3081, 2003.
28. Abujarad, F., G. Nadin, and A. Omar, "Clutter reduction and detection of landmine objects in ground penetrating radar using singular value decomposition (SVD)," *International Workshop on Advanced Ground Penetrating Radar*, 37–42, May 2–3, 2005.
29. Zhao, A., Y. Jiang, W. Wang, and X. Jiaotong, "Exploring independent component analysis for GPR signal processing," *PIERS Proceedings*, 750–753, Hangzhou, China, Aug. 22–26, 2005.
30. Moor, B. D., "The singular value decomposition and long and short spaces of noisy matrices," *IEEE Transactions on Signal Processing*, Vol. 41, No. 9, 2826–2838, 1993.
31. Konstantinides, K. and K. Yao, "Statistical analysis of effective singular values in matrix rank determination," *IEEE Transactions on Acoustics Speech and Signal Processing*, Vol. 36, No. 5, 757–763, 1998.
32. Trees, H. L. V., *Optimum Array Processing*, John Wiley, UK, 2003.
33. Wax, M. and T. Kailath, "Detection of signals by information theoretic criteria," *IEEE Transactions on Acoustics Speech Signal Processing*, Vol. 33, No. 2, 387–392, 1985.